

## **A comprehensive PDX gastric cancer collection captures cancer cell-intrinsic transcriptional MSI traits**

This is the peer reviewed version of the following article:

*Original:*

Corso, S., Isella, C., Bellomo, S.E., Apicella, M., Durando, S., Migliore, C., et al. (2019). A comprehensive PDX gastric cancer collection captures cancer cell-intrinsic transcriptional MSI traits. *CANCER RESEARCH*, 79(22), 5884-5896 [10.1158/0008-5472.CAN-19-1166].

*Availability:*

This version is available <http://hdl.handle.net/11365/1124862> since 2021-01-20T18:37:28Z

*Published:*

DOI:10.1158/0008-5472.CAN-19-1166

*Terms of use:*

Open Access

The terms and conditions for the reuse of this version of the manuscript are specified in the publishing policy. Works made available under a Creative Commons license can be used according to the terms and conditions of said license.

For all terms of use and more information see the publisher's website.

(Article begins on next page)

## **A comprehensive PDX gastric cancer collection captures cancer cell intrinsic transcriptional MSI traits.**

Simona Corso<sup>1,2</sup>, Claudio Isella<sup>2</sup>, Sara E. Bellomo<sup>2</sup>, Maria Apicella<sup>2</sup>, Stefania Durando<sup>2</sup>, Cristina Migliore<sup>1,2</sup>, Stefano Ughetto<sup>1,2</sup>, Laura D'Errico<sup>1,2</sup>, Silvia Menegon<sup>2</sup>, Daniel Moya-Rull<sup>1,2</sup>, Marilisa Cargnelutti<sup>2</sup>, Tania Capelo<sup>2#</sup>, Daniela Conticelli<sup>1,2</sup>, Jessica Giordano<sup>1,2</sup>, Tiziana Venesio<sup>2</sup>, Antonella Balsamo<sup>2</sup>, Caterina Marchiò<sup>2,3</sup>, Maurizio Degiuli<sup>4</sup>, Rossella Reddavid<sup>4</sup>, Uberto Fumagalli<sup>5§</sup>, Stefano De Pascale<sup>5§</sup>, Giovanni Sgroi<sup>6</sup>, Emanuele Rausa<sup>6</sup>, Gian Luca Baiocchi<sup>7</sup>, Sarah Molino<sup>7</sup>, Filippo Pietrantonio<sup>8,9</sup>, Federica Morano<sup>8</sup>, Salvatore Siena<sup>9,10</sup>, Andrea Sartore-Bianchi<sup>9,10</sup>, Maria Bencivenga<sup>11</sup>, Valentina Mengardo<sup>11</sup>, Riccardo Rosati<sup>12</sup>, Daniele Marrelli<sup>13</sup>, Paolo Morgagni<sup>14</sup>, Stefano Rausei<sup>15¶</sup>, Giovanni Pallabazzer<sup>16</sup>, Michele De Simone<sup>2</sup>, Dario Ribero<sup>2</sup>, Silvia Marsoni<sup>2‡</sup>, Antonino Sottile<sup>2</sup>, Enzo Medico<sup>1,2</sup>, Paola Cassoni<sup>3</sup>, Anna Sapino<sup>2,3</sup>, Eirini Pectasides<sup>17</sup>, Aaron R. Thorner<sup>18</sup>, Anwesha Nag<sup>18</sup>, Samantha D. Drinan<sup>18</sup>, Bruce M. Wollison<sup>18</sup>, Adam J. Bass<sup>17</sup> and Silvia Giordano<sup>1,2</sup>.

<sup>1</sup>Department of Oncology, University of Torino, Candiolo, Italy; <sup>2</sup>Candiolo Cancer Institute, FPO-IRCCS, Candiolo, Italy; <sup>3</sup>Department of Medical Sciences, University of Torino, Italy; <sup>4</sup>Department of Oncology, University of Torino, Orbassano, Italy; <sup>5</sup>Chirurgia Generale 2, Spedali Civili, Brescia, Italy; <sup>6</sup>Surgical Oncology Unit, Surgical Science Department, ASST Bergamo Ovest, Treviglio (BG), Italy; <sup>7</sup>Department of Clinical and Experimental Sciences, Surgical Clinic, University of Brescia, Italy; <sup>8</sup>Medical Oncology Department, Fondazione IRCCS Istituto Nazionale dei Tumori, Milan, Italy; <sup>9</sup>Department of Oncology and Hemato-oncology, University of Milan, Italy; <sup>10</sup>Niguarda Cancer Center, Grande Ospedale Metropolitano Niguarda, Milan, Italy; <sup>11</sup>First Department of General Surgery, Borgo Trento Hospital, University of Verona, Italy; <sup>12</sup>Gastroenterological Surgery Unit, IRCCS San Raffaele Hospital, Vita-Salute University, Milan,

Italy; <sup>13</sup>Department of Medicine, Surgery and Neurosciences, Unit of General Surgery and Surgical Oncology, University of Siena, Italy; <sup>14</sup>Pathology Unit, Morgagni-Pierantoni Hospital, Forlì, Italy. <sup>15</sup>Department of Surgery, University of Insubria, Varese, Italy; <sup>16</sup>Esophageal Surgery Unit, Medical University of Pisa, Italy; <sup>17</sup>Department of Medical Oncology, Dana-Farber Cancer Institute, Boston, MA; <sup>18</sup> Center for Cancer Genome Discovery (CCGD) Dana-Farber Cancer Institute, Boston, MA.

#Current Affiliation: FATH - Pole of pharmacology and therapeutics; IREC - Institute of Experimental and Clinical Research; UCL - Université Catholique de Louvain, Woluwe-Saint-Lambert, Belgium.

§Current Affiliation: Chirurgia dell'Apparato Digerente – European Institute of Oncology IRCCS – Milan, Italy.

¥ Current Affiliation: Department of Surgery, ASST Valle Olona, Gallarate, Varese, Italy

‡Current Affiliation: IFOM - The FIRC Institute of Molecular Oncology, Milan, Italy

**Correspondence:** Silvia Giordano and Simona Corso

Department of Oncology, University of Torino; Candiolo Cancer Institute, FPO-IRCCS, Strada Provinciale 142, Candiolo, 10060 (Torino), Italy. Phone: +39 011 9933233/8; Fax: +39 011 9933225; e-mail: [silvia.giordano@unito.it](mailto:silvia.giordano@unito.it); [simona.corso@unito.it](mailto:simona.corso@unito.it)

**Keywords:** gastric cancer, MSI, PDX, organoids, precision medicine

**Running Title:** MSI signature derived from a gastric cancer PDX platform

## **Grant support**

This work was funded by the Italian Association for Cancer Research (AIRC), IG 20210 to SG and IG 16819 to EM; Fondazione Piemontese per la Ricerca sul Cancro (FPRC, ONLUS) 5X1000 Min.Salute 2013 to A.Sottile; FPRC 5X1000 2014 Min. Salute to SG; FPRC 5X1000 2015 Min. Salute to SG and EM; FPRC 5X1000 2015 Min. Salute “Strategy” to SG; Ricerca Corrente 2019, Min. Salute to A.Sapino; Fondazione AIRC under 5 per Mille 2018 - ID. 21091 program – P.I. Bardelli Alberto, G.L. Medico Enzo to EM. Genomic sequencing was supported by the Schottenstein Fund for Gastric Cancer Research to ABass.

## **Disclosures**

All institutional and national guidelines for the care and use of laboratory animals were followed.

**Conflict of Interest:** The authors declare that they have no conflict of interest.

**Transcript Profiling:** Array data are deposited in GSE98708 and GSE128459

<https://www.ncbi.nlm.nih.gov/geo/query/acc.cgi?token=snsqycqynfyhful&acc=GSE98708>

<https://www.ncbi.nlm.nih.gov/geo/query/acc.cgi?acc=GSE128459>

**Additional information:** Word Count: 5182 words; 5 Figures.



## ABSTRACT

Gastric cancer (GC) is the world's third leading cause of cancer mortality. In spite of significant therapeutic improvements, the clinical outcome for patients with advanced GC is poor; thus, the identification and validation of novel targets is extremely important from a clinical point of view. We generated a wide, multi-level platform of GC models, comprising 100 patient-derived xenografts (PDXs), primary cell lines and organoids. Samples were classified according to their histology, microsatellite stability (MS), Epstein-Barr virus status, and molecular profile. This PDX platform is the widest in an academic institution and it includes all the GC histologic and molecular types identified by TCGA. PDX histopathological features were consistent with those of patients' primary tumors and were maintained throughout passages in mice. Factors modulating grafting rate were histology, TNM stage, copy number gain of tyrosine kinases/KRAS genes and MS status. PDX and PDX-derived cells/organoids demonstrated potential usefulness to study targeted therapy response. Finally, PDX transcriptomic analysis identified a cancer cell intrinsic MSI signature, which was efficiently exported to gastric cancer, allowing the identification -among MSS patients- of a subset of MSI-like tumors with common molecular aspects and significant better prognosis. In conclusion, we generated a wide gastric cancer PDX platform, whose exploitation will help identify and validate novel 'druggable' targets and optimize therapeutic strategies. Moreover, transcriptomic analysis of GC PDXs allowed the identification of a cancer cell intrinsic MSI signature, recognizing a subset of MSS patients with MSI transcriptional traits, endowed with better prognosis.

**Significance:** This study reports a multi-level platform of gastric cancer PDXs and identifies a MSI gastric signature that could contribute to the advancement of precision medicine in gastric cancer.

## INTRODUCTION

Gastric cancer (GC) is the fifth most common cancer and the third leading cause of cancer mortality in the world(1). From a histologic point of view, according to Lauren's classification, it can be divided in three main subtypes: intestinal, characterized by a glandular or papillary structure, frequently originating from intestinal metaplasia; diffuse, showing a poorly cohesive tissue architecture; mixed, presenting areas of both intestinal and diffuse histology. The TCGA analysis has recently proposed a molecular classification of this disease(2), recognizing four different genetic subtypes: Epstein Barr Virus positive (EBV, 9%), microsatellite instable (MSI, 22%), chromosomal instable (CIN, 50%) and genomically stable (GS, 20%). Each subtype is characterized by specific genomic alterations, many of which potentially targetable.

In spite of the increased molecular knowledge of GC, only one targeted therapy directed against molecular alterations of tumor cells has been approved so far, namely treatment with Trastuzumab in tumors displaying HER2 amplification(3). Indeed, most Phase III clinical trials evaluating molecular drugs in GC failed, suggesting the need of a more accurate patient selection and of pre-clinical models to assist clinical development of novel therapeutic strategies(3-10).

The cancer models that better recapitulate the biological characteristics of human tumors are, at present, Patient-Derived Xenografts (PDXs). These models are obtained by subcutaneous or orthotopic implantation in immunodeficient mice of small pieces of human tumors which are propagated in order to obtain cohorts of animals bearing the same tumors on which preclinical trials (xenotrials) can be performed (11,12). Xenotrials can be used to: i) validate altered genes as tumor drivers *–id est*, possible therapeutic targets-; ii) directly compare treatments targeting the same genetic lesions; iii) identify biomarkers of sensitivity/resistance; iv) compare the effect of different co-occurring genetic alterations on the therapeutic response. Indeed, some of these studies performed in PDXs have generated important preclinical information that led to the execution of successful clinical trials(13). Moreover, experience derived from co-clinical trials, where treatments

have been performed both in patients and in the corresponding PDXs, has shown the power of this approach(14,15).

Due to the low prevalence of many genetic lesions, however, these studies can be successfully performed only if a large number of PDXs is available. For this reason we generated a wide gastro-esophageal PDX platform (to our knowledge the widest in an academic institution), encompassing all the histological and molecular subtypes, also including *in vitro*-derived material, such as primary cell lines and organoids. We believe that this multilevel platform, rapidly and continuously growing, represents an invaluable resource to validate the effectiveness of inhibiting already known drivers, to perform preclinical studies comparing different therapeutic approaches, to identify new targets and to investigate mechanisms of resistance to treatment. The final goal is to generate knowledge to be translated in clinical trials which can eventually improve the prognosis of this deadly disease.

## **MATERIALS AND METHODS**

### **PDX generation**

Gastric PDX generation was performed as described in(16). Details are reported in Suppl. Material. All animal procedures adhered to the ‘Animal Research: Reporting of In Vivo Experiments’ (ARRIVE) standards and were approved by the Ethical Commission of the Candiolo Cancer Institute (Candiolo, Torino, Italy), and by the Italian Ministry of Health. All patients provided written informed consent; samples were collected and the study was conducted under the approval of the Review Boards of all the Institutions. The study was done in accordance with the principles of the Declaration of Helsinki, the International Conference on Harmonization and Good Clinical Practice guidelines and GDPR (General Data Protection Regulation).

### **GC Primary cell lines culture and organoids**

GC primary cells were derived from PDXs as described in (17). Gastric cancer organoids were derived as described in (18). The genetic identity of the *in vitro*-derived material with the original tumor has been verified by short tandem repeat profiling (Cell ID, Promega). Mycoplasma testing was performed upon culture setting.

### **PDX xenotrials**

GTR0503 PDXs were passaged and expanded for 2 generations until production of a cohort of 40 mice. Established and randomized tumors (average volume 300 mm<sup>3</sup>) were treated for the indicated days with the following regimens, (either single agent or combination): vehicle (saline) per os; Cetuximab 20 mg/Kg, twice weekly ip; JNJ-605 50mg/kg, daily, per os. N=6. Tumor size was evaluated once-weekly by caliper measurements and approximate volume of the mass was calculated using the formula  $4/3\pi(D/2)(d/2)^2$ , where d is the minor tumor axis and D is the major tumor axis. GTR0233 and GTR0455 PDXs were expanded for 4 and 2 generations respectively, until the production of 20 mice for each GC model. Established tumors were randomized (average

volume 250 mm<sup>3</sup>) and treated for the indicated days with vehicle (saline) or Trastuzumab 30 mg/kg, weekly, through intra-peritoneal injection.

### **Organoid transplantation**

Gastric cancer organoids were s.c. injected into flanks of NOD/SCID mice. For each organoid line three mice were used, each receiving into one flank organoids derived from 24 wells of a 24 well plate (approximately  $2 \times 10^6$  cells/mouse) in 100  $\mu$ l Matrigel.

### **Imaging**

H&E was performed on 3  $\mu$ m thick tissue sections. Organoids were embedded in Richard-Allan Scientific™ HistoGel™ Specimen Processing Gel (Thermo Fisher Scientific) according to manufacturer instructions, fixed in formalin, processed according to standard methods and finally embedded in paraffin.

Images were captured with the AxiovisionLe software (Zeiss) using an Axio Zeiss Imager 2 microscope (Zeiss).

### **Cell viability assay**

Cells were seeded in 96-well plastic culture plates (3000/well), in the presence of the indicated drugs or vehicle (DMSO) for 6 days. Cell viability was measured by using the Cell Titer-Glo Luminescent Cell Viability Assay (Promega).

### **EBV evaluation**

Detection and quantification of EBV DNA were performed using the EBV Q-PCR Alert KIT (ELITechGroup S.p.A.). The real time amplification assay was carried out on ABI 7300 Real-Time PCR System instrument (Applied Biosystems, USA). PDXs were classified as described in (16): EBV high (with high EBV burden, >1000, Equivalent EBV Genomes/reaction (gEq), EBV intermediate (75-1000 gEq) or EBV low/neg (<75 gEq). Tumors scored as EBV high or intermediate were considered as EBV positive.

### **MSI evaluation**

MS status was evaluated with the MSI Analysis System version 1.2 kit (Promega). MSI analysis was performed according to the manufacturer's directions. The pathologist interpreted microsatellite instability at  $\geq 2$  mononucleotide loci as MSI, instability at a single mononucleotide locus and no instability at any of the loci tested as microsatellite stable (MSS).

### **Genomic sequencing**

DNA extracted from PDX models along with a sample of normal germline DNA from each patient were utilized for next generation sequencing. Using standard methods, Illumina sequencing libraries were generated and subjected to hybrid capture with a focused targeted bait set of 243 genes selected based upon their alteration in prior studies of gastroesophageal cancer (19). Details are reported in Suppl. Methods.

### **Microarray data generation, preprocessing and differential expression analysis**

Synthesis of cDNA and biotinylated cRNA (from 500ng total RNA) was performed using the IlluminaTotalPrep RNA Amplification Kit (Ambion), according to the manufacturer's protocol. Quality assessment and quantitation of cRNAs were performed with Agilent RNA kits on a Bioanalyzer 2100 (Agilent). Hybridization of cRNAs (750ng) was carried out using Illumina Human 48k gene chips (Human HT-12 V4 BeadChip). Array washing was performed by Illumina High Temp Wash Buffer for 10' at 55°C, followed by staining using streptavidin-Cy3 dyes (Amersham Biosciences). Hybridized arrays were stained and scanned in a Beadstation 500 (Illumina) and HiScanSQ. Data were analyzed as described in (16). Details are reported in Suppl. Methods. Array data are deposited in GSE98708 and GSE128459.

### **Statistics**

#### *Statistical Analysis*

Statistical testing for pharmacological experiment was performed with GraphPAD PRISM Software 8.0, using the test indicated in Figure Legends. Statistical significance: ns= not significant; \*p <0,05; \*\*p <0,01; \*\*\*p <0,001.

## RESULTS

### Patients characteristics.

Gastro-esophageal cancer patients were consecutively enrolled in 15 different Italian Hospitals in which the GEA (Gastro-Esophageal Annotated platform) project has been approved. We included in the study a total of 349 gastro-esophageal cancer patients (Figure 1A), whose tumors were molecularly characterized and whose follow up was recorded. Detailed patient characteristics are reported in Suppl. Table S1. Median patients' age was 71 (range: 32-90 years), with a male to female ratio of 1.97 (226:115). 19.1% of the tumors were located in the gastro-esophageal junction (GEJ) or in the upper part of the stomach (6.9%), 19.4% in the middle part and 49.6% in the lower part; 5% derived from residual tissue of a previous gastrectomy. From a histologic point of view, according to Lauren classification, intestinal, diffuse and mixed carcinomas were 66.2%, 29.3% and 4.5%, respectively. Differentiation (defined by grading) was high in 2.6%, moderate in 27.3% and poor in 70.1% of the cases. In 38.9% of patients, tumors were diagnosed at stages I/II, and in 61.1% at stages III/IV. 21.3% of patients received neoadjuvant chemotherapy before surgery.

Gastro-esophageal carcinomas were also analysed for EBV and MS status: 10% of tumors had an intermediate/high EBV burden, while 17.6% showed microsatellite instability (Suppl. Table S1).

### Establishment of PDX models.

From the 349 patients included in the study we established 145 PDX models in NOD-SCID mice, with a success rate of 42% (in the range of what previously reported(20)). The histological analysis of PDXs revealed that around 30% of the mice developed a human-derived lymphoproliferative disease (monoclonal and EBV+), characterized by a mutational burden and an expression profile distinct from gastric adenocarcinomas and endowed with very fast growth kinetics(16). Lymphoma onset did not correlate neither with the level of lymphocyte infiltration, nor with the histotype of the original gastric tumor, nor with patient outcome(16).

The 100 PDXs which developed GC (Figure 1A) showed histopathological features consistent with those of patients' primary tumors that were maintained throughout different passages in mice (Figure 1B,C). Indeed, hierarchical clustering analysis of the transcriptome confirmed that PDXs were significantly more similar to their corresponding primary tumors than to unmatched pairs (Figure 1D). These data suggest that PDXs maintained the identity of their pre-implantation surgical counterparts, both at histological and transcriptional levels. Only in few cases, primary tumors with mixed histology generated either intestinal or diffuse PDXs (Figure 1C), probably as a consequence of an unbalanced representation of the mixed component in the transplanted primary.

The mean latency period of tumor growth (from implant to the appearance of a palpable tumor) was 73.5 days (median: 61 days; range: 27-237 days). In 83% of the PDXs, the latency period shortened in the following serial passages (average engraftment time at second passage: 50 days; median: 38 days; range 15-414 days), (Suppl. Table S2).

### **Factors influencing PDX generation**

To investigate potential factors influencing PDX generation we evaluated both patient and tumor characteristics. We did not observe any statistically significant correlation between engraftment and patient characteristics such as age or gender. Quite surprisingly, previous neoadjuvant chemotherapy did not significantly affect tumor take rate (Suppl. Table S2). Concerning the pathological characteristics of the tumors, while tumor site and EBV status did not correlate with engraftment (Suppl. Table S2), histology turned out to be relevant. Not surprisingly, intestinal type tumors showed a significantly higher grafting than diffuse type tumors (intestinal tumors engrafted in 36.52% of the cases vs 11.34% of diffuse ones,  $P < 0.0001$ ; Suppl. Table S2 and Figure 1E). Other factors influencing PDX generation were TNM stage, copy number gain of genes coding for Receptor Tyrosine Kinases (RTKs)/KRAS and MSI status. Concerning TNM, stage III/IV tumors showed a higher engraftment rate ( $P < 0.05$ ) (Suppl. Table S2 and Figure 1E). Tumors with a RTK/KRAS amplification ( $\geq 8$  gene copies, a threshold considered biologically and clinically



relevant(21,22)) positively correlated with engrafting. Indeed, 43.47% of primary tumors presenting RTK/KRAS amplification engrafted vs 26.75% of the non-amplified ones ( $P<0.05$ ) (Suppl. Table S2). Finally, MSI tumors had an engraftment rate significantly higher than MSS tumors (55.93% vs 23.64%,  $P<0.0001$ ); this resulted in the enrichment of MSI PDXs (34%) compared to the donor patient population (18%), (Figure 1E).

## PDX Characterization

As shown in Figure 1, the PDX platform captures all the GC subtypes, even if it is enriched in intestinal histology, MSI status, high stage and RTKs/KRAS amplification compared to the donor tumors. As mentioned above, MSI tumors showed an engraftment rate higher than MSS ones. Interestingly, while some “stable” microsatellites were still present in primary tumors, they were completely lost in the corresponding PDXs (Suppl. Figure S1A, B). To investigate if this was due to the loss of human stroma in the PDXs (which was present in the primary tumors, possibly contributing the “normal” allele) or to the *in vivo* selection of a more unstable subpopulation, we generated organoids from primary tumors and analysed them after few passages. As already described also by others (23), gastric cancer organoids achieved very high tumor purity, with few or no stroma component (Suppl. Figure S2A). Indeed, organoid analysis showed the absence of the MSS component (Suppl. Figure S1B), thus strengthening the hypothesis that the “stable” component is contributed by the human stroma.

As previously mentioned, the TCGA consortium identified four major genomic subtypes of gastric cancer, associated with EBV positivity, MSI status, Chromosomal Instability (CIN) and Genomic stability (GS), respectively. The integration of data obtained by genomic sequencing, EBV testing and MS evaluation allowed PDX molecular categorization. As shown in Figure 2A, all the subtypes were captured in the platform, even if the PDX collection displayed a higher occurrence of MSI samples. The analysis of the most frequent genetic alterations (mutations and CNV, Figure 2B,C) revealed that the PDX platform captures the molecular heterogeneity of human gastric tumors.

Indeed, all the most frequent mutations/CNVs reported by TCGA(2) are present in the platform. As the platform comprises several models bearing alterations in druggable genes of the RTK/RAS and RTK/PI(3)K signalling pathways (Figure 2D and Suppl. Table S3), it is an optimal instrument to perform ‘xenotrials’ verifying the effect of the inhibition of these targets and optimizing the therapeutic approach. PDX models data and metadata will be openly available in PDX Finder (<https://doi.org/10.1093/nar/gky984>, [pdxfinder.org](https://pdxfinder.org)) and in the EurOPDX data portal (<http://dataportal.europdx.eu>) that will be constantly updated with the newly generated models.

### **‘Xenotrials’ with GC PDXs mimic patient response to targeted therapies.**

In order to verify if our GC PDXs reliably recapitulate patients’ response to targeted drugs, we looked for established PDX in which the corresponding donor patients had been treated with Trastuzumab (at present, the only molecular therapy targeting tumor cells approved in GC). Only one patient bearing HER2+ GC, from which we derived a PDX, underwent Trastuzumab treatment (in combination with chemotherapy), showing primary resistance to this therapy (progressive disease, according to RECIST 1.1 criteria; Figure 3A, upper panel). The corresponding PDX, named GTR0455, was serially passaged in mice until six tumor-bearing animals were produced per experimental group. When xenografts reached an average volume of  $\sim 250 \text{ mm}^3$ , mice were randomized into 2 cohorts, and treated for one month with either vehicle (saline) or Trastuzumab. To assess tumor response to therapy, we measured tumor volume and used a ‘RECIST 1.1-like’ classification, inspired by clinical criteria, already described for PDX models (24): (i) partial response (PR) was defined as a decrease of at least 50% in the tumor volume, taking as reference the baseline volume; (ii) progressive disease (PD) was defined as at least 35% increase in tumor volume; (iii) intermediate tumor variations were defined as stable disease (SD); (iv) complete response (CR) was the disappearance of the tumor. In accordance with the clinical history of the donor patient (Figure 3A), all the Trastuzumab-treated GTR0455 mice were resistant to treatment and experienced disease progression (Figure 3A, lower panel). Importantly, we observed response

to Trastuzumab in other HER2-positive PDXs (e.g. in GTR0233, reported in Figure 3B), but we could not compare it to the donor patients, who were never treated with Trastuzumab since they never relapsed.

### **Generation and characterization of PDX-derived cell lines and organoids**

To perform *in vitro* studies, from a fraction of the PDXs we derived both primary cell lines and organoids, obtaining 34 (from 72 samples) 2D primary cell lines and 37 (from 51 samples) organoids (Figure 1A; for details see the M&M section). Histologic analysis of the organoids confirmed that they maintained the characteristics of the corresponding primary tumors and of the PDXs (representative examples are shown in Figure 4A). Interestingly, when organoids were reinjected in mice, they originated tumors very similar to the corresponding PDXs (Suppl. Figure S2B). To further characterize the *in vitro* derivatives, we profiled their gene expression. As shown in Figure 4B, hierarchical clustering analysis of the transcriptome confirmed that both primary cells and organoids very closely recapitulated the PDX of origin.

To confirm the experimental value of these models for testing the responsiveness to targeted drugs matching actionable genomic alterations, we performed *in vitro* and *in vivo* experiments. As an experimental and representative model, we chose a case (GTR0503) displaying amplification (30 copies, Figure 4C) and overexpression (Figure 4D) of the MET oncogene, encoding the receptor for the Hepatocyte Growth Factor (HGF). Treatment of primary cells with MET tyrosine Kinase inhibitors (JNJ-605, a MET specific kinase inhibitor; Crizotinib, a multikinase inhibitor) resulted in partial inhibition of cell viability. As we showed that in gastric cancer EGFR activation can mediate resistance to MET inhibitors (17), we co-treated the cells with MET and EGFR inhibitors. The dual MET/EGFR targeting resulted both in a sustained inhibition of downstream targets and in a profound impairment of cell growth (Figures 4D,E). To validate *in vivo* these results, the original tumor was serially passaged to originate 4 independent treatment cohorts (6 PDXs/group): (i) vehicle (placebo); (ii) JNJ-605 (a selective MET inhibitor); (iii) Cetuximab; (iv) JNJ-605 +

Cetuximab. As shown in Figure 4F, the GTR0503 PDX showed a partial response upon MET inhibition but the addition of the anti-EGFR drug (*per se* ineffective) resulted in a more intense and prolonged response. These results confirm the experimental predictive value of the *in vitro*-derived models but they also show that the preclinical experiments performed in PDXs can be more informative, providing information also on the long-term response to the treatment.

### **Identification of a cancer cell intrinsic MSI signature which predicts disease outcome**

Even if, overall, gastric cancer is endowed with poor prognosis, prognostic heterogeneity has been observed in patients bearing tumors of different molecular subtypes. Indeed, Cristescu and collaborators have shown that patients with MSI tumors display the best prognosis, in line with what observed in other cancer types(25). It is in fact believed that the high mutational burden present in MSI tumors promotes leucocyte infiltration, leading to activation of the immune system(26).

Although the molecular landscape of MSI vs MSS tumors has already been investigated in other tumor types(27), not much is known in the case of gastric cancer. We thus took advantage of the GC PDX platform to identify genes modulated in MSI cancer cells. In fact, as the stromal component of PDXs is of murine origin, this analysis allows the identification of the molecular differences restricted to the human tumor cells. Focusing on genes expressed by cancer cells, we identified a MSI signature composed of 123 genes with strong differential regulation (adjusted  $p$ -val  $< 0.05$ ,  $|\log_2| > 1$ ), subdivided in two modules: 23 of them were upregulated and 100 downregulated (Suppl. Table S4, upper part and Figure 5A). As expected, MLH1 was among the genes strongly downregulated in MSI samples. Interestingly, GSEA analysis showed that most of the dysregulated genes are involved in metabolism and that MSI tumors displayed an increased Warburg phenotype (Suppl. Table S4, lower part).

To predict the MSI status we calculated a Gastric MSI score as the weighted average of the expression of the two modules (Figure 5B, left panel; ROC AUC=0.971). To validate the identified

Gastric MSI score we interrogated the largest available gastric cancer gene expression dataset(2) and found that this signature predicted microsatellite instability with high specificity (ROC AUC=0.93; Figure 5B, middle panel). Interestingly, our MSI signature outperformed the previously published MSI signature(27) derived from the analysis of primary human colon cancers which displayed lower prediction values both in the PDX collection and in the TCGA cohort (PDX AUC=0.86, TCGA ROC AUC=0.89; Suppl. Figure S3).

Our Gastric MSI score was successfully validated also in the ACRG dataset(25) (AUC=0.804; Figure 5B, right panel). As this dataset is annotated with disease free survival (DFS) of gastric cancer patients, we verified if our MSI score was associated with a prognostic value. As shown in Figure 5C, left panel, the MSI score was indeed able to identify patients with lower recurrence rate (log rank chi square  $p < 0.005$ ). Similar results were obtained also in the GSE26253 (432 patients) and in our PDX cohort as well (IRCC, 65 patients) (Figure 5C, middle and right panel, respectively). In the ACRG dataset (for which the MS status is available), we observed that a portion of MSS samples was endowed with MSI transcriptional traits; strikingly, these patients displayed better prognosis, compared to the other MSS patients (log rank chi square  $p < 0.05$ ; Figure 5D, left panel). Moreover, also in the MSI subtype it was possible to discriminate between patients harbouring high or low levels of MSI-like score; despite not reaching significant values (possibly due to the low number of samples), the two populations showed different overall survival (Figure 5D, right panel).

Altogether these results demonstrate that the transcriptomic analysis of GC PDXs allowed the identification of a cancer cell intrinsic MSI signature, generated without taking in consideration the contribution of leucocyte infiltration. This signature can be efficiently exported to gastric cancer, allowing the identification -among MSS patients- of a subset of MSI-like tumors with common molecular assets and significant better prognosis.

## DISCUSSION

Oncology has recently and rapidly moved from a phenotype-based empirical management to a more personalized approach centred on treatment of patients according to their tumor genetic profile. This approach has led to significant results in neoplasms such as lung, breast and colorectal carcinomas, where driver genes to which tumor cells are addicted have been identified. Unfortunately, this approach has been quite limited in GC where only two drugs, Trastuzumab and ramucirumab, respectively targeting HER2 and VEGFR, have been approved so far(3). For this reason, there is an urgent need for studies able to identify targetable drivers in this neoplasm.

Patient-derived xenografts have proved to be a crucial experimental model to discover new targets in several solid tumors and to be endowed with a high predictive value(11,12). Although PDXs possess notable advantages, they do have limitations such as their low engraftment rate and poor propensity to metastasize, the presence of a microenvironment which is different from that of the primary tumor, the existence of intratumor heterogeneity and the engraftment in mice which have a severely compromised immune system. Nevertheless, PDX models represent a significant challenge for oncology research as they reflect human tumor biology more accurately than any other existing models.

We thus generated a platform of gastric cancer PDXs to identify and validate targets and optimize molecular treatments in this disease. To our knowledge, our gastric PDX platform is the widest developed in an academic institution. As most of the molecular alterations that can be investigated as possible therapeutic targets are present only in a minority of gastric cancer samples, the availability of a high number of PDX models is critical for the success of these studies. From the TCGA analysis, in fact, we can infer that the frequency of molecular alterations of targetable kinases such as EGFR, FGFR2 and MET is around or lower than 10%(2). Since in many described samples either the identified mutations are not activating or the gene of interest is amplified at a level not sufficient to induce addiction of cancer cells, the number of PDXs suitable to perform

preclinical trials is even lower. The availability of a wide PDX platform is thus critical to perform studies on a significant number of models sharing the same genetic lesions.

The preclinical value of such a platform relies on some requirements: (i) it has to include the whole spectrum of the described histotypes; (ii) the PDXs must recapitulate the histopathologic, biologic and genetic features of their donor tumors. In this work we show that our platform includes intestinal, diffuse and mixed subtypes, as described by Lauren's classification. Even though other groups did not obtain PDXs from tumors of the diffuse subtype(20) we succeeded in establishing PDXs also from this histotype, that maintained their pathologic characteristics. Their under representation is probably due to the fact that these tumors are characterized by the presence of an abundant stroma, containing relatively few cancer cells that are not sufficient to confer a high engraftment rate. Overall, the generated PDX models retained the principal characteristics of donor tumors, including fine tissue structure and subtle microscopic details (gland architecture, mucin production etc.). Gene expression profile was well conserved among the original tumors, PDXs and the *in vitro*-derived material. Moreover, the integration of genetic analysis, EBV evaluation and microsatellite status showed that all the molecular types identified by the TCGA classification were indeed represented. Finally, the genetic analysis revealed that all the most frequent gastric cancer-based genomic alterations identified in public consortia were well represented in our platform. All together, these results demonstrate that the platform captures the heterogeneity of human gastric tumors.

The overall engraftment rate of our PDXs (42%) was in line with that described by other authors(20). However, we observed that some characteristics of the tumor could sensibly affect it. Indeed, the histology (intestinal vs diffuse), the stage (advanced vs early), the presence of alterations in receptor tyrosine kinases/KRAS genes and microsatellite stability status (MSI vs MSS) significantly increased tumor engraftment, which has been correlated with tumor aggressiveness.



An important feature of PDX models is their ability to mimic patients' response to targeted therapies (12). For GC PDXs this is particularly difficult to be verified as, at present, the only approved molecular therapy targeting tumor cells is Trastuzumab, an anti-HER2 monoclonal antibody administered to HER2 positive, metastatic GC patients, which represent a relative small fraction (10-20%) of GC patients(3). Only one of our HER2+ PDXs has been derived from a patient who underwent Trastuzumab treatment and showed primary resistance; notably, the established PDX completely recapitulated the absence of response observed in the corresponding patient. . Importantly, we observed response to Trastuzumab treatment in other HER2-positive PDXs, but unfortunately we could not compare it to the donor patients, as they have not been treated with the drug since they never relapsed. However, these results confirm also in PDXs the association between HER2 amplification and sensitivity to Trastuzumab, known to occur in patients.

As a complement to the PDX platform, we also derived *in vitro* primary cell lines and organoids, to allow the execution of biochemical and pharmacological studies. Also in this case, histological and gene expression analyses were concordant with those performed in the corresponding PDXs. As already described by others, gastric cancer organoids grown in Matrigel achieve a very high tumor purity, containing few or no stroma (23). As recently highlighted (28), this allows a clear delineation of the cancer cell molecular and transcriptional features, otherwise confounded by normal cells contamination. At the same time, the loss of the stroma component represents a limit. Novel techniques to obtain cancer organoids containing fibroblasts and immune components have been recently proposed (29,30); in the future, it will be extremely interesting to add these novel models in our organoid collection. Despite the absence of stromal component, 3D cultures are anyway different from classical 2D cultures, as organoids better mimics the physical features and the architecture of the original (solid) tumors; indeed, cancer cells maintain the original morphology and polarity. On the other hand, 2D are less expensive and are an easier experimental system (especially to perform high-throughput assays). For this reason, we decided to derive both 2D and



3D primary cultures from gastric PDXs. Interestingly, for some models we could obtain both 2D and 3D derivatives while, in other cases we generated only one of the two.

As already demonstrated in other systems, we showed that the pharmacological response obtained in primary cells and in organoids paralleled what observed *in vivo*(23,31,32). However, at least for what concerns molecular therapies targeting Receptor Tyrosine Kinases (RTKs), studies performed in animals can be more informative as they allow the evaluation of the efficacy of long lasting treatments, show the effectiveness of treatment in delaying/preventing relapse and are of invaluable value in discovering molecular mechanisms sustaining resistance. Another important point is that targeted drugs often show a different activity *in vitro* and *in vivo*, particularly in the case of some monoclonal antibodies. Moreover, *in vitro* models are devoid of tumor stroma, which can mediate resistance to tyrosine kinase inhibitors(33).

Finally, we interrogated our platform to gain more insight in MSI tumors. The first observation is that even if MSI gastric cancers display a better outcome, they are intrinsically more aggressive, as testified by their engraftment rate, more than two folds higher than that of MSS tumors. The oximorum between these two contradictory observations is probably due to the fact that MSI tumors are characterized by a high mutational burden which in humans promotes the activation of the immune system; this, in turn, likely mitigates the aggressiveness of the tumor. As our PDXs have been generated in non-immunocompetent animals, the inhibitory activity of the immune system is lost and, thus, MSI tumors can probably unleash their full aggressiveness.

Both computational methods that analyse next generation sequencing data (NGS) and transcriptomic analysis have been developed to detect MSI(27,34,35).We decided to exploit the transcriptome of our PDXs to generate a signature able to discriminate MSI and MSS gastric tumors. The use of PDX-derived material has the enormous advantage of taking in consideration only cancer cell-derived material as the stroma is of murine origin and can thus be easily subtracted during the analysis. The possibility to ignore the stromal contribution is very important in gastric cancer where the two main subtypes –intestinal and diffuse- strongly differ for the relative amount

of the stromal component which is significantly more abundant in the latter. In particular, MSI tumors are usually very rich in immune cells whose gene expression importantly affects the transcriptome. The transcriptomic analysis performed on our PDX cohort allowed the identification of a cancer cell intrinsic MSI signature. In line with our data that show a cell intrinsic difference between MSI and MSS cancer cells, recent papers have demonstrated that WRN silencing is lethal in MSI cells but not in MSS ones, in absence of any influence of the microenvironment (36-39). A pillar of current precision oncology is to deconvolve cancer cell-intrinsic oncogenic dependencies and drug resistance mechanisms from microenvironment-driven ones. Exploration of cancer cell transcriptome in PDX takes advantage of species-specific sequences to achieve such deconvolution. Our signature was validated in our and in two wide external datasets. In the ACRG dataset we verified that our MSI score was able to identify patients with lower recurrence rate; notably, it also identified some patients bearing MSS tumors endowed with MSI transcriptional traits who displayed better prognosis. This observation is important from a clinical point of view as it would allow the identification of cases lacking the genetic MSI characteristics but displaying an MSI like signature, thus broadening the therapeutic base for Immuno or other PARP-type drugs.

In sum, we have generated a wide gastric cancer PDX platform which covers in a reliable manner all the gastric cancer subtypes. Its deep molecular annotation as well as the generation of *in vitro*-derived material (primary cells and organoids) represents an invaluable instrument to identify new molecular targets and to optimize therapeutic approaches in gastric cancer.

## ACKNOWLEDGEMENTS

We thank the colleagues of GIRCG ('Gruppo Italiano Ricerca Carcinoma Gastrico') for their support; R.Porporato, D.Cantarella, B.Martinoglio, M.Buscarino and M.Montone for technical support with gene array, Real Time PCR and Cell-ID; I.Sarotto, D.Balmativola, E.Maldi for pathological analysis; animal facility employees; F.Fesi, S.Saponaro, M.Mangioni for EBV analysis; Dr. Natale for organizing follow up data; L.Trusolino and A.Bertotti for helpful scientific discussion. SG, SC, EM, CI are EuroPDX Consortium members.

## REFERENCES

1. Ferlay J, Soerjomataram I, Dikshit R, Eser S, Mathers C, Rebelo M, *et al.* Cancer incidence and mortality worldwide: Sources, methods and major patterns in GLOBOCAN 2012. *Int J Cancer* **2015**;136:E359-86
2. Network CGAR. Comprehensive molecular characterization of gastric adenocarcinoma. *Nature* **2014**;513:202-9
3. Bang YJ, Van Cutsem E, Feyereislova A, Chung HC, Shen L, Sawaki A, *et al.* Trastuzumab in combination with chemotherapy versus chemotherapy alone for treatment of HER2-positive advanced gastric or gastro-oesophageal junction cancer (ToGA): a phase 3, open-label, randomised controlled trial. *Lancet* **2010**;376:687-97
4. Corso S, Giordano S. How Can Gastric Cancer Molecular Profiling Guide Future Therapies? *Trends Mol Med* **2016**;22:534-44
5. Satoh T, Xu RH, Chung HC, Sun GP, Doi T, Xu JM, *et al.* Lapatinib plus paclitaxel versus paclitaxel alone in the second-line treatment of HER2-amplified advanced gastric cancer in Asian populations: TyTAN--a randomized, phase III study. *J Clin Oncol* **2014**;32:2039-49
6. Hecht JR, Bang YJ, Qin SK, Chung HC, Xu JM, Park JO, *et al.* Lapatinib in Combination With Capecitabine Plus Oxaliplatin in Human Epidermal Growth Factor Receptor 2-Positive Advanced or Metastatic Gastric, Esophageal, or Gastroesophageal Adenocarcinoma: TRIO-013/LOGiC-A Randomized Phase III Trial. *J Clin Oncol* **2016**;34:443-51
7. Tabernero J, Hoff PM, Shen L, Ohtsu A, Shah MA, Cheng K, *et al.* Pertuzumab plus trastuzumab and chemotherapy for HER2-positive metastatic gastric or gastro-oesophageal junction cancer (JACOB): final analysis of a double-blind, randomised, placebo-controlled phase 3 study. *Lancet Oncol* **2018**;19:1372-84
8. Lordick F, Kang YK, Chung HC, Salman P, Oh SC, Bodoky G, *et al.* Capecitabine and cisplatin with or without cetuximab for patients with previously untreated advanced gastric cancer (EXPAND): a randomised, open-label phase 3 trial. *Lancet Oncol* **2013**;14:490-9
9. Waddell T, Chau I, Cunningham D, Gonzalez D, Okines AF, Frances A, *et al.* Epirubicin, oxaliplatin, and capecitabine with or without panitumumab for patients with previously untreated advanced oesophagogastric cancer (REAL3): a randomised, open-label phase 3 trial. *Lancet Oncol* **2013**;14:481-9
10. Dutton SJ, Ferry DR, Blazeby JM, Abbas H, Dahle-Smith A, Mansoor W, *et al.* Gefitinib for oesophageal cancer progressing after chemotherapy (COG): a phase 3, multicentre, double-blind, placebo-controlled randomised trial. *Lancet Oncol* **2014**;15:894-904
11. Byrne AT, Alf  rez DG, Amant F, Annibali D, Arribas J, Biankin AV, *et al.* Interrogating open issues in cancer precision medicine with patient-derived xenografts. *Nat Rev Cancer* **2017**
12. Hidalgo M, Amant F, Biankin AV, Budinsk   E, Byrne AT, Caldas C, *et al.* Patient-derived xenograft models: an emerging platform for translational cancer research. *Cancer Discov* **2014**;4:998-1013
13. Sartore-Bianchi A, Trusolino L, Martino C, Bencardino K, Lonardi S, Bergamo F, *et al.* Dual-targeted therapy with trastuzumab and lapatinib in treatment-refractory, KRAS codon 12/13 wild-type, HER2-positive metastatic colorectal cancer (HERACLES): a proof-of-concept, multicentre, open-label, phase 2 trial. *Lancet Oncol* **2016**
14. Chen Z, Cheng K, Walton Z, Wang Y, Ebi H, Shimamura T, *et al.* A murine lung cancer co-clinical trial identifies genetic modifiers of therapeutic response. *Nature* **2012**;483:613-7
15. Nardella C, Lunardi A, Patnaik A, Cantley LC, Pandolfi PP. The APL paradigm and the "co-clinical trial" project. *Cancer Discov* **2011**;1:108-16
16. Corso S, Cargnelutti M, Durando S, Menegon S, Apicella M, Migliore C, *et al.* Rituximab Treatment Prevents Lymphoma Onset in Gastric Cancer Patient-Derived Xenografts. *Neoplasia* **2018**;20:443-55
17. Apicella M, Migliore C, Capel  a T, Menegon S, Cargnelutti M, Degiuli M, *et al.* Dual MET/EGFR therapy leads to complete response and resistance prevention in a MET-amplified gastroesophageal xenopatient cohort. *Oncogene* **2016**

18. Miyoshi H, Stappenbeck TS. In vitro expansion and genetic modification of gastrointestinal stem cells in spheroid culture. *Nat Protoc* **2013**;8:2471-82
19. Pectasides E, Stachler MD, Derks S, Liu Y, Maron S, Islam M, *et al.* Genomic Heterogeneity as a Barrier to Precision Medicine in Gastroesophageal Adenocarcinoma. *Cancer Discov* **2018**;8:37-48
20. Choi YY, Lee JE, Kim H, Sim MH, Kim KK, Lee G, *et al.* Establishment and characterisation of patient-derived xenografts as preclinical models for gastric cancer. *Sci Rep* **2016**;6:22172
21. Gomez-Martin C, Plaza JC, Pazo-Cid R, Salud A, Pons F, Fonseca P, *et al.* Level of HER2 gene amplification predicts response and overall survival in HER2-positive advanced gastric cancer treated with trastuzumab. *J Clin Oncol* **2013**;31:4445-52
22. Suda K, Murakami I, Katayama T, Tomizawa K, Osada H, Sekido Y, *et al.* Reciprocal and complementary role of MET amplification and EGFR T790M mutation in acquired resistance to kinase inhibitors in lung cancer. *Clin Cancer Res* **2010**;16:5489-98
23. Yan HHN, Siu HC, Law S, Ho SL, Yue SSK, Tsui WY, *et al.* A Comprehensive Human Gastric Cancer Organoid Biobank Captures Tumor Subtype Heterogeneity and Enables Therapeutic Screening. *Cell Stem Cell* **2018**;23:882-97.e11
24. Bertotti A, Migliardi G, Galimi F, Sassi F, Torti D, Isella C, *et al.* A molecularly annotated platform of patient-derived xenografts ("xenopatients") identifies HER2 as an effective therapeutic target in cetuximab-resistant colorectal cancer. *Cancer Discov* **2011**;1:508-23
25. Cristescu R, Lee J, Nebozhyn M, Kim KM, Ting JC, Wong SS, *et al.* Molecular analysis of gastric cancer identifies subtypes associated with distinct clinical outcomes. *Nat Med* **2015**;21:449-56
26. Samstein RM, Lee CH, Shoushtari AN, Hellmann MD, Shen R, Janjigian YY, *et al.* Tumor mutational load predicts survival after immunotherapy across multiple cancer types. *Nat Genet* **2019**;51:202-6
27. Tian S, Roepman P, Popovici V, Michaut M, Majewski I, Salazar R, *et al.* A robust genomic signature for the detection of colorectal cancer patients with microsatellite instability phenotype and high mutation frequency. *J Pathol* **2012**;228:586-95
28. Chan AS, Yan HHN, Leung SY. Breakthrough Moments: Organoid Models of Cancer. *Cell Stem Cell* **2019**;24:839-40
29. Neal JT, Li X, Zhu J, Giangarra V, Grzeskowiak CL, Ju J, *et al.* Organoid Modeling of the Tumor Immune Microenvironment. *Cell* **2018**;175:1972-88.e16
30. Dijkstra KK, Cattaneo CM, Weeber F, Chalabi M, van de Haar J, Fanchi LF, *et al.* Generation of Tumor-Reactive T Cells by Co-culture of Peripheral Blood Lymphocytes and Tumor Organoids. *Cell* **2018**;174:1586-98.e12
31. Crystal AS, Shaw AT, Sequist LV, Friboulet L, Niederst MJ, Lockerman EL, *et al.* Patient-derived models of acquired resistance can identify effective drug combinations for cancer. *Science* **2014**;346:1480-6
32. van de Wetering M, Francies HE, Francis JM, Bounova G, Iorio F, Pronk A, *et al.* Prospective derivation of a living organoid biobank of colorectal cancer patients. *Cell* **2015**;161:933-45
33. Apicella M, Giannoni E, Fiore S, Ferrari KJ, Fernández-Pérez D, Isella C, *et al.* Increased Lactate Secretion by Cancer Cells Sustains Non-cell-autonomous Adaptive Resistance to MET and EGFR Targeted Therapies. *Cell Metab* **2018**;28:848-65.e6
34. Bonneville R, Krook MA, Kautto EA, Miya J, Wing MR, Chen HZ, *et al.* Landscape of Microsatellite Instability Across 39 Cancer Types. *JCO Precis Oncol* **2017**;2017
35. Hause RJ, Pritchard CC, Shendure J, Salipante SJ. Classification and characterization of microsatellite instability across 18 cancer types. *Nat Med* **2016**;22:1342-50
36. Behan FM, Iorio F, Picco G, Gonçalves E, Beaver CM, Migliardi G, *et al.* Prioritization of cancer therapeutic targets using CRISPR-Cas9 screens. *Nature* **2019**;568:511-6
37. Chan EM, Shibue T, McFarland JM, Gaeta B, Ghandi M, Dumont N, *et al.* WRN helicase is a synthetic lethal target in microsatellite unstable cancers. *Nature* **2019**;568:551-6
38. Kategaya L, Perumal SK, Hager JH, Belmont LD. Werner Syndrome Helicase Is Required for the Survival of Cancer Cells with Microsatellite Instability. *iScience* **2019**;13:488-97

39. Lieb S, Blaha-Ostermann S, Kamper E, Rippka J, Schwarz C, Ehrenhöfer-Wölfer K, *et al.* Werner syndrome helicase is a selective vulnerability of microsatellite instability-high tumor cells. *Elife* **2019**;8

## FIGURE LEGENDS

**Figure 1. The PDX platform captures all the GC subtypes, and it is enriched in intestinal histology, MSI status, high stage and RTKs/KRAS amplification compared to donor tumors.**

**A:** 349 fresh surgical gastric adenocarcinoma samples were subcutaneously implanted in NOD/SCID mice, generating 100 gastric PDXs; from a fraction of PDXs we derived 34 2D primary cell lines (from 72 samples) and 37 organoids (from 51 samples). **B.** Representative micrographs of three gastric adenocarcinomas featuring distinct growth-patterns. GTR0079 is a moderately differentiated gastric adenocarcinoma of intestinal type, showing a glandular architecture; the intestinal type GTR0165 adenocarcinoma displays also foci of mucin production; GTR0244 shows a diffuse growth-pattern. As illustrated, xenografted tumors retained the histopathologic characteristics of the original samples through passages. **C.** Caleydo plot showing the histological correlation between primary tumor and the corresponding PDX. The graph shows that in the vast majority of the cases there was a perfect match between the primary tumor and the PDX. **D.** Unsupervised hierarchical clustering analysis of the transcriptome performed on primary tumors and the corresponding PDXs. The analysis demonstrates that PDXs were significantly more similar to their corresponding primary tumors than to unmatched pairs. **E.** The graph illustrates the percentage of donor tumors (TUMOR, n=349) and of derived PDXs (PDX, n=100) for the following features: histology (intestinal, diffuse or mixed); MS status (MSI or MSS); stage (I/II or III/IV); RTK/KRAS copy number variation (CNV < or  $\geq 8$  copies).

**Figure 2. The PDX platform captures the molecular complexity of GC.** **A.** PDXs were categorized into the molecular subtypes identified by TCGA: Epstein–Barr virus (EBV)-positive, microsatellite instability (MSI), chromosomal instability (CIN) and genomically stable (GS). **B.** The 20 genes most frequently mutated in MSI tumors in the TCGA dataset (grey bars) and in MSI PDXs (blue bars). **C.** The 20 genes most frequently amplified/lost in non-MSI tumors according to TCGA (grey bars) and their alteration frequency in non-MSI PDXs (blue bars).

Amplifications are shown as positive frequencies; deletions as negative values. **D.** Mutations and copy-number changes for select genes belonging to RTK/RAS and RTK/PI(3)K signalling pathways are shown across MSI and MSS PDXs.

**Figure 3. ‘Xenotrials’ with GC PDXs mimic patient’s response to HER2 targeted therapy.**

**A.** Upper Part: summary of donor patient’s clinical history. The clinical course of the patient with HER2+ GC is summarized, with level of serum cancer antigen 19-9 (Ca 19.9) tumor marker shown throughout treatment (blue line). CEA tumor marker values are reported in red. Red-lined boxes indicate periods of administration of the indicated therapeutic agents. Blue vertical lines indicate timing of tumor specimen acquisition from surgical procedures or biopsies, as well as dates of tumor assessment by either CT scan or FDG-PET/CT scan. PD, progressive disease; PR, partial response, according to RECIST 1.1. BSC, Best Supportive Care. The patient showed primary resistance to Trastuzumab treatment. Lower Part: Spaghetti plot illustrating the xenotrial performed on the cohort of mice derived from PDX GTR0455, obtained from the above described donor patient. Individual lines represent, for each mouse, the percentage variation in tumor burden, from treatment start (day 0) to 4 weekly consecutive serial assessments. Blue lines: vehicle-treated mice; red lines: Trastuzumab-treated mice (30 mg/kg). The response in mice has been evaluated using RECIST 1.1-like criteria, highlighted in the magnification: progressive disease (PD):  $\geq 35\%$  increase from baseline; partial response (PR):  $\geq 50\%$  reduction from baseline; stable disease (SD): intermediate variations from baseline. As shown, all mice displayed progressive disease. **B.** Spaghetti plot (performed as in A) illustrating the xenotrial performed on the cohort of mice derived from the HER2 + PDX GTR0233. As shown, all mice displayed response to treatment.

**Figure 4. Generation and characterization of PDX-derived primary cell lines and organoids.**

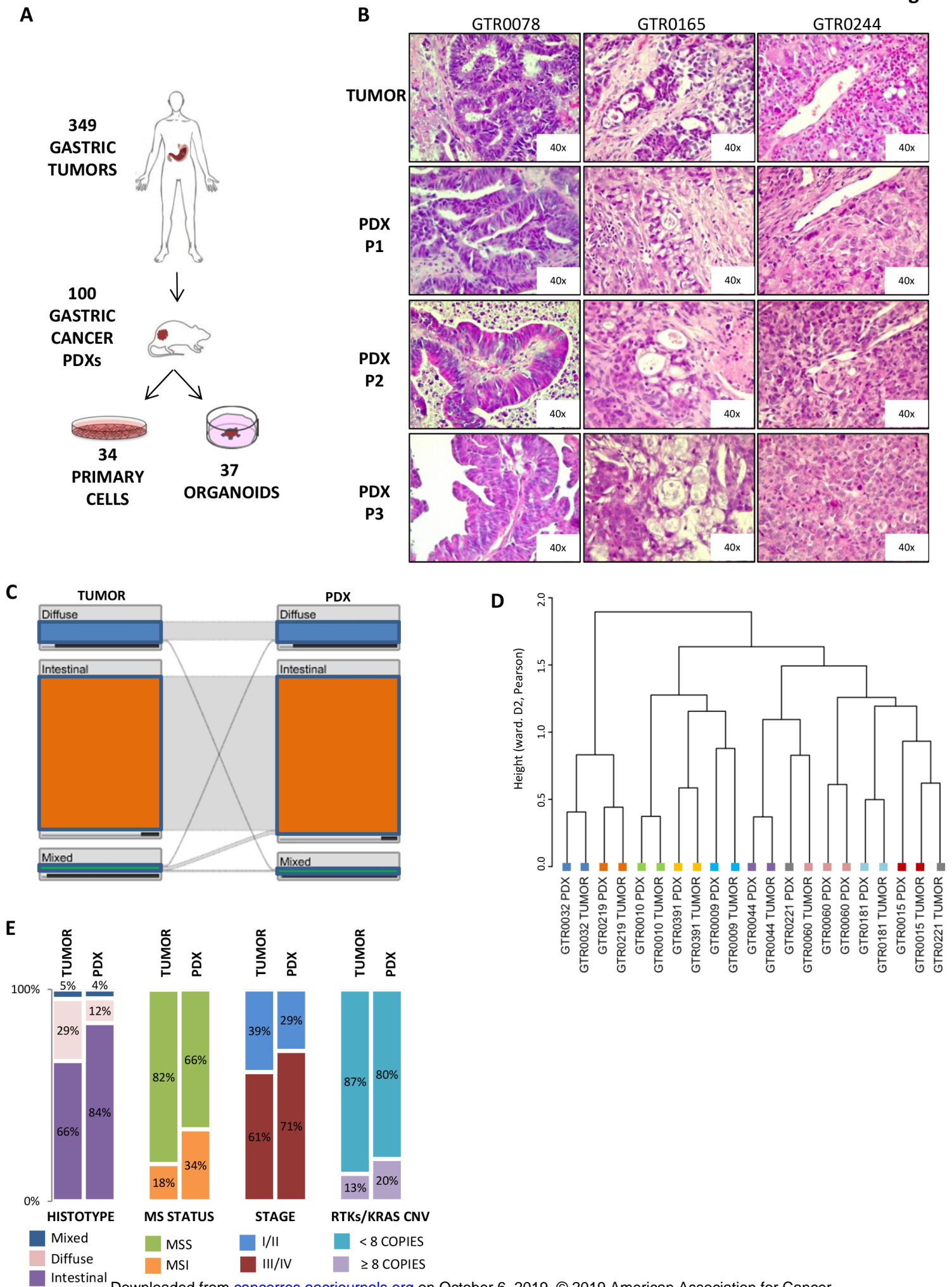
**A.** Representative H&E images and bright field microscopy of PDX-derived gastric tumor organoids, matched PDXs and primary tumors for intestinal (GTR0032 and GTR0062) and

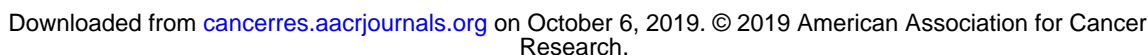


diffuse histotypes (GTR0263). **B.** Unsupervised hierarchical clustering analysis of the transcriptome performed on organoids (ORGA), primary cells (CELLS) and the corresponding PDXs. The analysis shows the perfect matching of PDXs and the corresponding *in vitro*-derivatives. **C.** qRT-PCR analysis of MET gene copy number in the original tumor (GTR0503), in the PDX and in the *in vitro* derived primary cells compared with the diploid cell line 293T. **D.** Western Blot analysis of MET, EGFR, AKT and MAPK expression and phosphorylation in GTR0503 cells untreated or treated with the indicated drugs (JNJ-605 250 nM, Crizotinib 250 nM, Lapatinib 250 nM for 2 hours; Cetuximab 10µg/ml for 16 hours). **E.** Cell viability assay performed on tumor-derived cells, upon treatment with the indicated drugs for 6 days. JNJ-605 (50nM); CRIZ: Crizotinib (50nM); CETUX: Cetuximab (1µg/ml). **F.** Tumor growth curves in the mice cohort derived from the GTR0503 patient treated with placebo (VEHICLE), the MET inhibitor JNJ-605 (50mg/kg, daily, per os) and Cetuximab (CETUX, 20 mg/Kg, twice weekly ip), alone or in combination, as indicated. N =6 mice for Vehicle, JNJ-605 and Cetuximab arms; N=5 for the combo arm. The arrow indicates treatment start. In C, E, F data are represented as mean + SD. \*\*\* p<0,001; ns= not significant. One-way ANOVA with Bonferroni multiple comparisons test has been used for panel E. Two-way ANOVA followed by Bonferroni multiple comparisons test has been used for panel F.

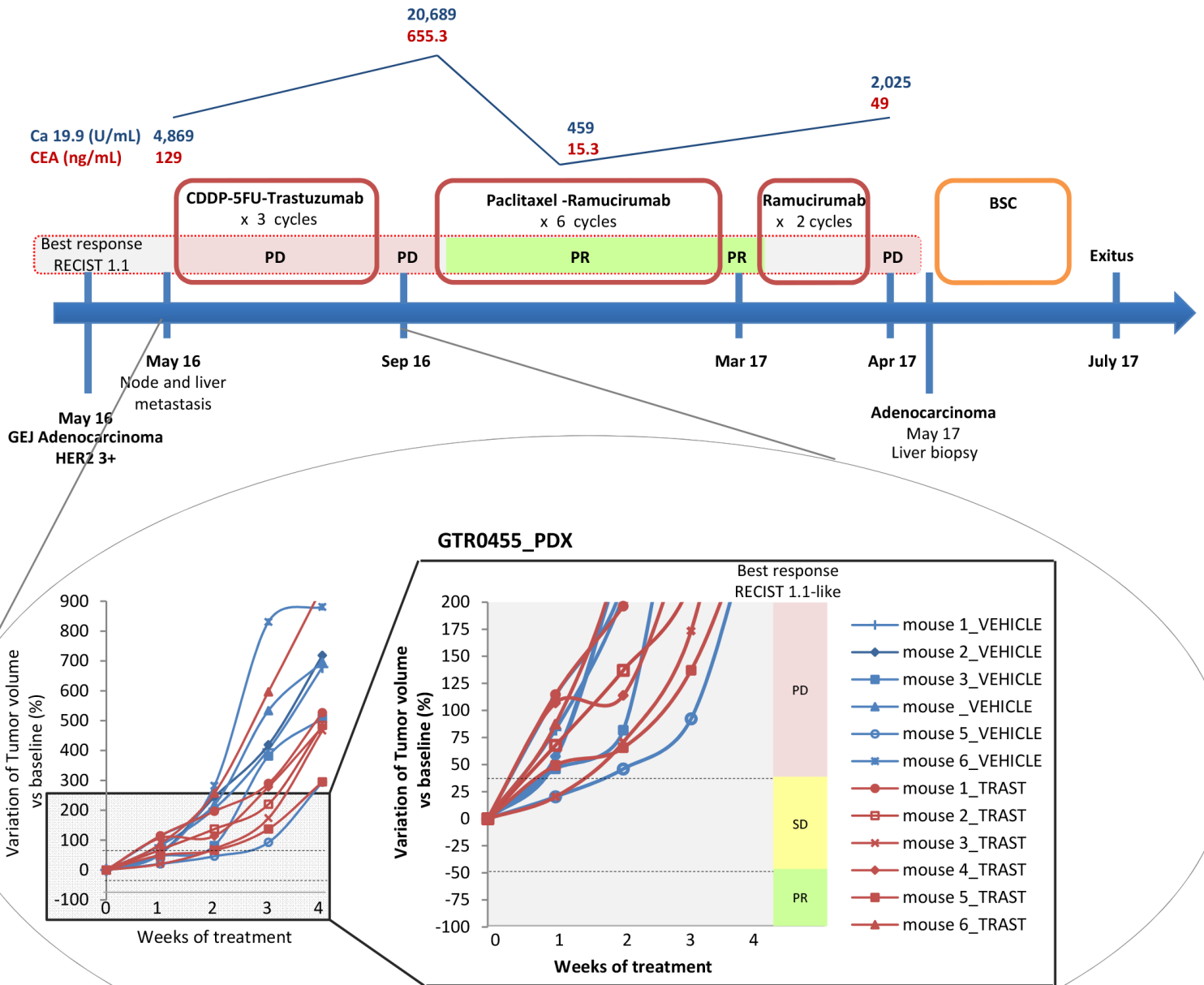
**Figure 5. PDX-derived MSI score predicts outcome in GC patients.** **A.** Heatmap representing log two ratio value of the MSI signature in the PDX collection; genetic MS status of the respective tumors is reported above (MSI tumors: black rectangles; MSS tumors: white rectangles). **B.** ROC curves of gastric MSI score predicting MSI genetic status in PDX (left panel), TCGA (middle panel) and ACRG (GSE66229) cohorts (right panel). **C.** Kaplan–Meier plot of DFS for MSI signature subtyping in prognostically annotated GC gene expression data sets: ACRG (GSE66229, left), GSE26253 (center) and IRCC (right). **D.** Kaplan–Meier plot of DFS for MSI signature subtyping in the ACRG MSS (left panel) and MSI (right panel) subsets.

**Figure 1**





A



B

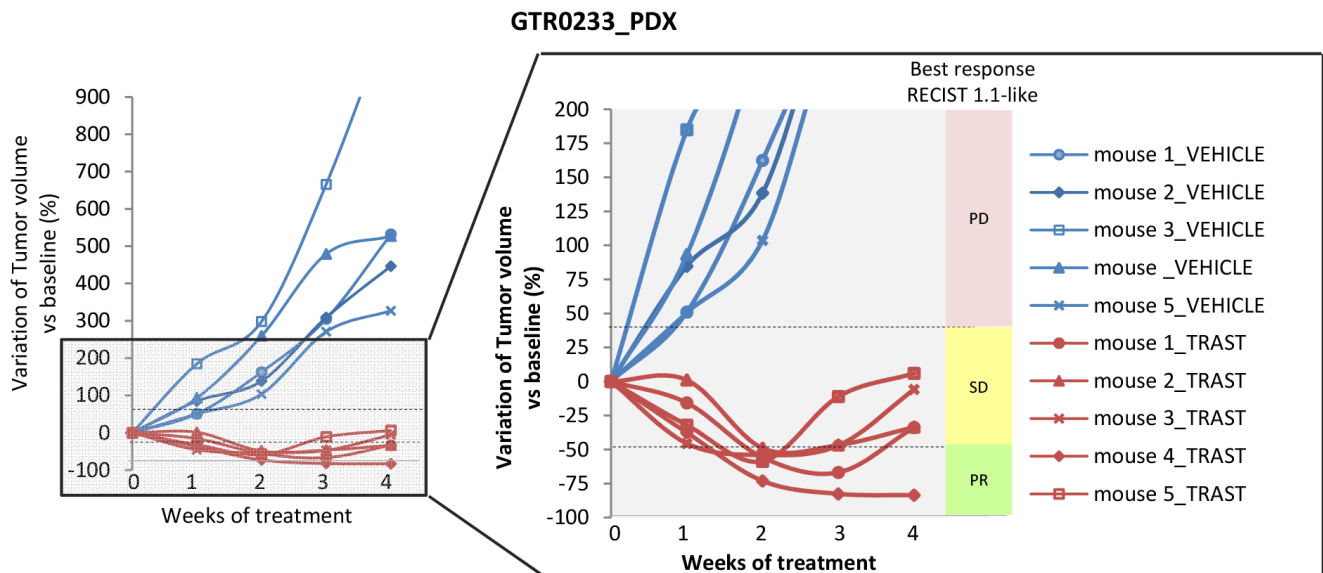
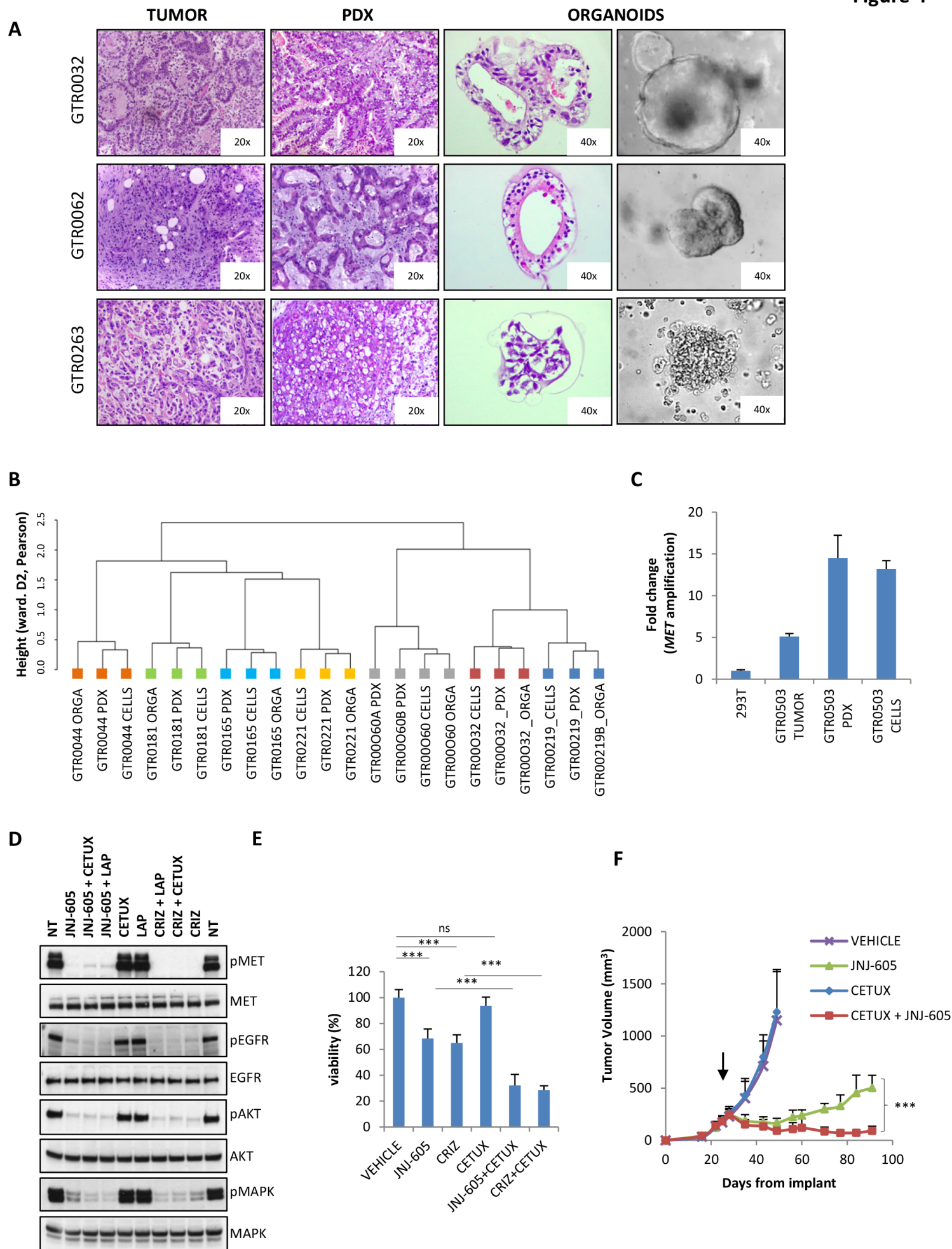
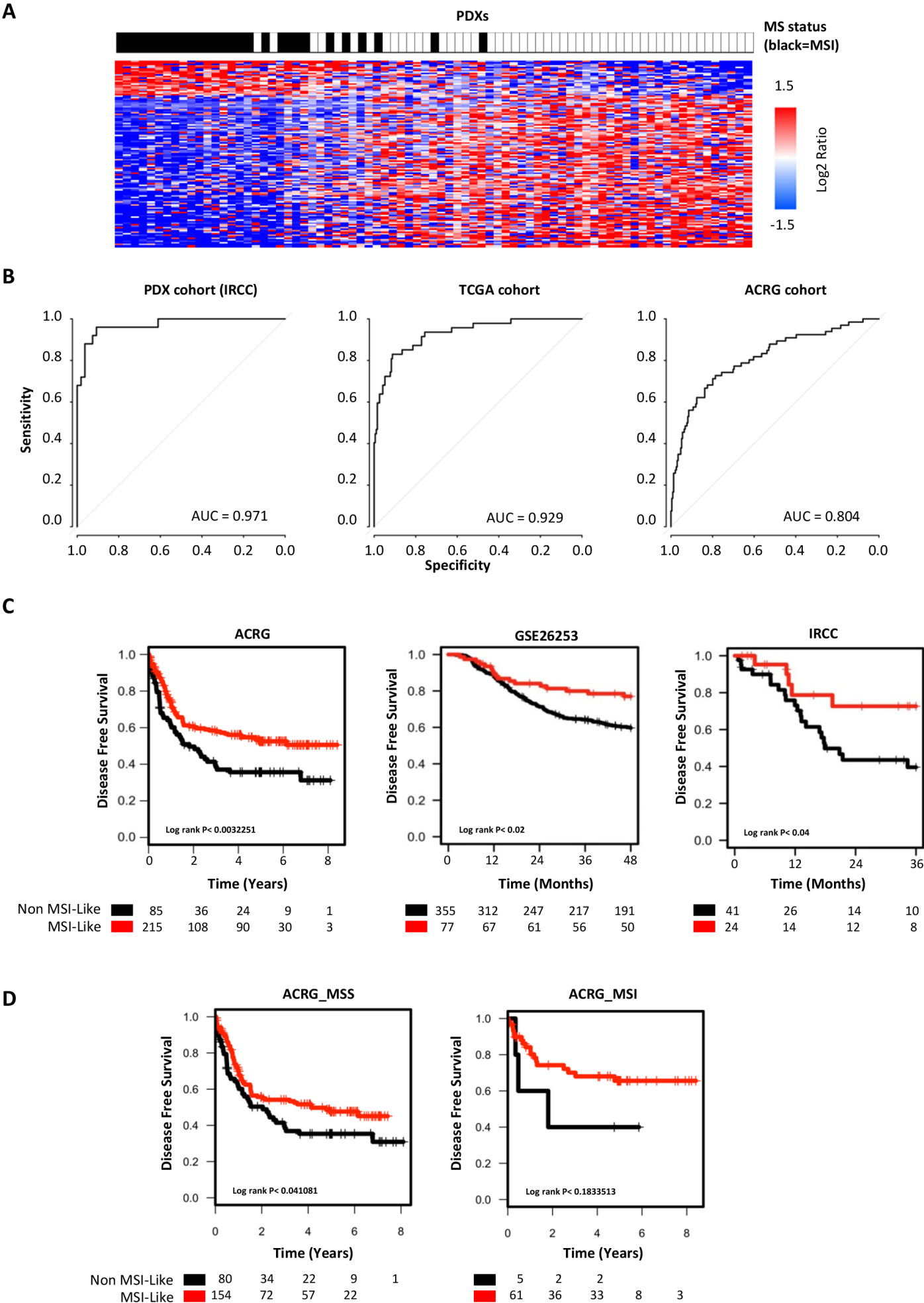




Figure 4





# Cancer Research

The Journal of Cancer Research (1916–1930) | The American Journal of Cancer (1931–1940)

## A comprehensive PDX gastric cancer collection captures cancer cell intrinsic transcriptional MSI traits.

Simona Corso, Claudio Isella, Sara E Bellomo, et al.

*Cancer Res* Published OnlineFirst October 4, 2019.

<b>Updated version</b>	Access the most recent version of this article at: doi: <a href="https://doi.org/10.1158/0008-5472.CAN-19-1166">10.1158/0008-5472.CAN-19-1166</a>
<b>Supplementary Material</b>	Access the most recent supplemental material at: <a href="http://cancerres.aacrjournals.org/content/suppl/2019/10/04/0008-5472.CAN-19-1166.DC1">http://cancerres.aacrjournals.org/content/suppl/2019/10/04/0008-5472.CAN-19-1166.DC1</a>
<b>Author Manuscript</b>	Author manuscripts have been peer reviewed and accepted for publication but have not yet been edited.

<b>E-mail alerts</b>	<a href="#">Sign up to receive free email-alerts</a> related to this article or journal.
<b>Reprints and Subscriptions</b>	To order reprints of this article or to subscribe to the journal, contact the AACR Publications Department at <a href="mailto:pubs@aacr.org">pubs@aacr.org</a> .
<b>Permissions</b>	To request permission to re-use all or part of this article, use this link <a href="http://cancerres.aacrjournals.org/content/early/2019/10/04/0008-5472.CAN-19-1166">http://cancerres.aacrjournals.org/content/early/2019/10/04/0008-5472.CAN-19-1166</a> . Click on "Request Permissions" which will take you to the Copyright Clearance Center's (CCC) Rightslink site.